THEORETICAL APPROACH TO THERMAL DECOMPOSITION PROCESS OF CHOSEN ANHYDROUS OXALATES

A. Koleżyński[1] and A. Małecki[2]*

[1]Copernicus Center for Interdisciplinary Studies, ul. Gronostajowa 3, 30-387 Cracow, Poland
[2]AGH University of Science and Technology, Faculty of Materials Science and Ceramics, Al. Mickiewicza 30 30-059 Cracow, Poland

The results of theoretical analysis of the properties of crystal structure and bonding in relation to thermal decomposition process in chosen anhydrous metal oxalates (Cd, Co, Zn) are presented. The methods used in this analysis – the Bader's quantum theory of atoms in molecules and bond order model (as defined by Cioslowski and Mixon), applied to topological properties of the electron density, obtained from DFT calculations performed by Wien2k package (full potential linearized augmented plane wave method), as well as Brown's bond valence model (bonds valences and strengths, and bond and crystal strains, calculated from crystal structure and bonds lengths data) are described.

Presented results allow us to state, that these methods, when used simultaneously, make possible the description and analysis of the crystal structure and bonding properties and give us the additional insight into its behavior during thermal decomposition process. The proposed theoretical approach can be considered as promising and reliable tool for theoretical analysis, allowing explanation and prediction of the properties of the structure and bonding and hence the most probable way of thermal decomposition process to take place in such structure.

Keywords: *bond order, bond strength thermal decomposition, bond valence, electron density topology, FP-LAPW ab initio calculations*

Introduction

Anhydrous metal oxalates β-MC_2O_4 (where *M* is Fe, Co, Ni, Zn, Cu – Kondrashev *et al.* [1]; Cd – Jeanneau *et al.* [2]) form the isostructural family with monoclinic unit cell $P2_1/n$, with similar cell parameters, arrangement of the MO_6 octahedra and oxalate anions, but different thermal decomposition to $M+2CO_2$, $MO+CO+CO_2$ or MCO_3+CO [3–11]. Despite many experimental results, there is still lack of consistent description and explanation of the origin and thermal decomposition path in given oxalate, but one can expect, that the main reasons of differences between oxalates behaviour during thermal decomposition is due to the differences in nature of chemical bonds in oxalates depending on a kind of metal atom and crystal structure. Thus theoretical study of fundamental features of electron density (topological analysis) and chemical bond (bond order, bond valence, bond strains, etc.) should in principle lead to the prediction of the way of thermal decomposition in given metal oxalates. In this paper, we propose one of possible theoretical approach, the theoretical analysis based on the topological properties of electron density obtained from first principles calculations (Bader's quantum theory of atoms in molecules [12] formalism) together with Pauling's 'electrostatic va-

lence rule' [13] based structural consideration of bond valence, bond strength and strains associated with deviation of given structure from ideal one [14], which in our opinion can give us additional insight into the thermal decomposition process and help not only to explain thermal decomposition path in given oxalate, but also – to some extent – to predict such most probably path for the compounds for which experimental results are unavailable.

In this paper we present the results of the theoretical studies undertaken for chosen anhydrous oxalates (zinc, cadmium and cobalt oxalates), decomposing thermally via different way, i.e. to $M+2CO_2$ (cadmium oxalate), $MO+CO+CO_2$ (zinc oxalate) and to both these types of products (cobalt oxalate). The detailed analysis of the obtained results for these oxalates can be found elsewhere [15–17], thus in this paper have focused on the comparison of respective results of the bonds topological properties, bond orders and bond strains and their relation to the way of thermal decomposition process.

Computational details

The DFT calculations of the electronic structure for crystals under considerations, have been performed us-

---

*   Author for correspondence: malecki@uci.agh.edu.pl

ing WIEN2k FP-LAPW (full potential linearized augmented plane wave method) package [18], within density functional theory (DFT) formalism [19–24]. In all cases, for reliable comparison purposes, the calculations has been performed for 500 k-points (7×7×8 mesh within the irreducible Brillouin zone), cut-off parameter Rk_{max}=7.5 and GGA-PBE exchange-correlation potential [25]. The values of muffin-tin radii (R_i) has been set to [a.u.]: M – 1.7, O – 1.08, C – 1.08. Similarly, for all structures the identical convergence criteria for SCF calculations, namely $\Delta E_{SCF} \leq 10^{-5}$ Ry for total energy and $\Delta \rho_{SCF} \leq 10^{-5}$ e for electron density topology analysis has been chosen.

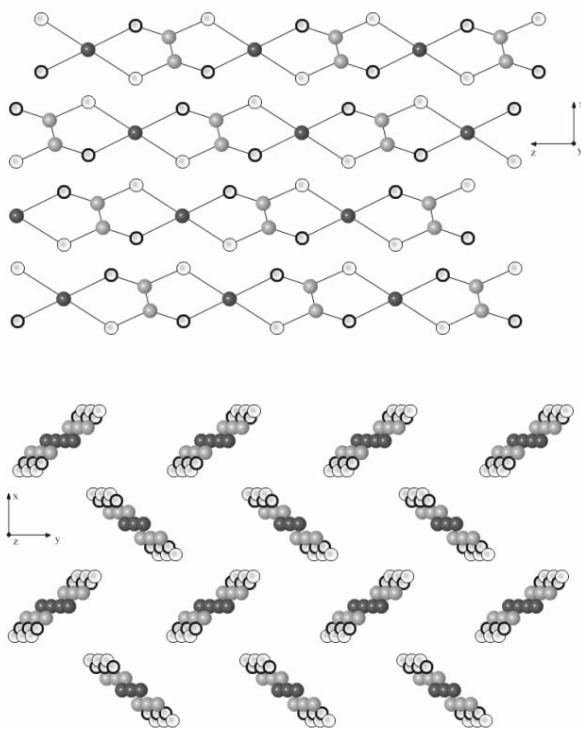On the basis of the SCF electron density distribution in crystal cell, the topological properties of bond critical points (within Bader's quantum theory of atoms in molecules [12] formalism, based on the gradient dynamical system analysis) have been calculated.

Anhydrous metal oxalate structure

The crystal structure of anhydrous metal oxalates (zinc, cadmium and cobalt) can be described as built from chains –C_2O_4–M–C_2O_4–M– (Fig. 1), or alternatively as layered material, formed by cationic layers built from corner-shared MO_6 octahedra, linked together via bidentate chelating oxalate groups. Each metal atom is surrounded by six oxygen atoms, all belonging to oxalate groups: two O_1 and four O_2 atoms, forming distorted octahedron (Fig. 2) with 3 different M–O distances. All octahedra are connected by corners; in each metal octahedron, all four O_2 atoms are shared by two octahedra, belonging to neighboring chains, almost perpendicular to each other (Fig. 2).

One can find detailed description of the crystal structure for zinc, cadmium and cobalt oxalates in [15, 16, 26], respectively. The crystal structure parameters used in DFT calculations are listed in Table 1.

Results

Electron density topology

The electron density distribution data obtained from SCF calculations where used in Bader's QTAiM anal-

Fig. 1 Anhydrous metal oxalate chain structure projected onto *xz* and *xy* planes. In the lower figure, the plane is slightly rotated in x direction to show the chains spatial orientation (chains are parallel to *z* axis). Black, gray and shaded circle dots represents metal, carbon and oxygen atoms respectively (there are two kinds of shaded circles – normal and bold one, for two symmetrically non-equivalent oxygen atoms)
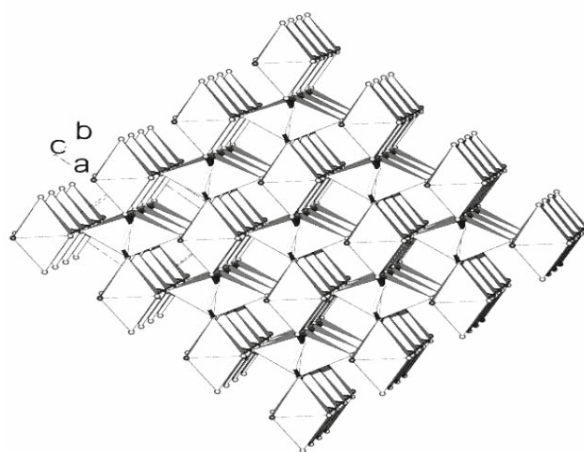

Fig. 2 Anhydrous metal oxalate crystal structure

Table 1 Experimental crystal structure data for anhydrous zinc [1], cadmium [2] and cobalt [26] oxalates

Structure	Space group	a/Å	b/Å	c/Å	β/°	V/Å^3
ZnC_2O_4	P2$_1$/n	5.831	5.123	5.331	113.20	146.37
CdC_2O_4	P2$_1$/n	5.826	5.252	5.832	113.86	163.19
CoC_2O_4	P2$_1$/c	5.3182	5.4183	6.4858	120.245	161.43

ysis of electron density topology. The parameters characterizing respective bond critical points, as well as based on them bond orders have been calculated and the results are presented in Tables 2–4. Bader and co-workers have shown, that the gradient vector field, derived from the scalar electron density distribution allows us to partition the space into adjoint basins occupied by atomic cores, separated by electron density gradient zero-flux surfaces. The main advantage of such analysis is the possibility of calculating the properties of the electron density in special points (the so-called critical points) for which a gradient of the electron density $\nabla\rho(r)$ is equal to zero. There are four different types of critical points, but the most important for our purposes is bond critical point (BCP), which indicates the existence of a chemical bond between given atoms. Every bond critical point, can be described by its position, electron density in this point, three eigenvalues, λ_i (i=1, 2, 3) of Hessian ma-

trix of the electron density $\rho(r)$ and Laplacian $\nabla^2\rho(r)$, defined as a trace of Hessian matrix and these parameters make up powerful tools to classify a given structure: two negative eigenvalues of the Hessian matrix (λ_1 and λ_2) measure the degree of contraction of electron density in directions perpendicular to each other and normal to the bond towards the BCP, while a positive eigenvalue (λ_3) gives us a quantitative indication of the degree of contraction in direction parallel to the bond and from the BCP towards each of the neighbouring nuclei. The electronic charge is locally concentrated in the region of the BCP (covalent or polarized bonds) when negative eigenvalues dominate (this is characterized by large $\rho(r)$ values, $\nabla^2\rho(r)<0$ and $|\lambda_1|/\lambda_3>1$). If positive eigenvalue dominates, the electronic density is locally concentrated at each atomic basin, the interaction is classified as closed shell and it is typical of highly ionic bonds, hydrogen bonds, and van der Waals interactions (relatively low

Table 2 Bond lengths R, Hessian eigenvalues λ_1–λ_3, electron density $\rho(r)$ and Laplacian $\nabla^2\rho(r)$ in BPC, calculated for anhydrous zinc oxalate

ZnC_2O_4		$R/\text{Å}$	$\lambda_1/\text{Å}^{-5}$	$\lambda_2/\text{Å}^{-5}$	$\lambda_3/\text{Å}^{-5}$	$\nabla^2\rho(r)/\text{Å}^{-5}$	$\rho(r)/\text{e}/\text{Å}^{-3}$	ε
r_1	Zn–O_1	1.9465	–3.2558	–3.2414	16.0598	0.6163	9.5630	0.0045
r_2	Zn–O_2^i	2.0548	–2.4172	–2.3767	11.7123	0.4990	6.9160	0.0170
r_3	Zn–O_2^{ii}	2.3174	–1.1021	–1.0806	5.4561	0.2714	3.2730	0.0198
r_4	C_1–O_1	1.1551	–35.5465	–33.3052	74.0330	3.2041	5.1960	0.0673
r_5	C_1–O_2^i	1.4114	–14.5945	–12.5895	9.9916	1. 9010	–17.1920	0.1593
r_6	C_1–C_2	1.5398	–13.0136	–11.9340	10.2856	1.7168	–14.6620	0.0905

Table 3 Bond lengths R, Hessian eigenvalues λ_1–λ_3, electron density $\rho(r)$ and Laplacian $\nabla^2\rho(r)$ in BPC, calculated for anhydrous cadmium oxalate

CdC_2O_4		$R/\text{Å}$	$\lambda_1/\text{Å}^{-5}$	$\lambda_2/\text{Å}^{-5}$	$\lambda_3/\text{Å}^{-5}$	$\nabla^2\rho(r)/\text{Å}^{-5}$	$\rho(r)/\text{e}/\text{Å}^{-3}$	ε
r_1	Cd–O_1	2.2421	–1.9034	–1.8809	9.9578	6.1740	0.4324	0.0118
r_2	Cd–O_2^i	2.3210	–1.5207	–1.5023	8.0275	5.0030	0.3608	0.0121
r_3	Cd–O_2^{ii}	2.3469	–1.4211	–1.3763	7.4587	4.6630	0.3344	0.0315
r_4	C_1–O_1	1.2462	–24.9187	–23.3980	34.4861	–13.8280	2.6474	0.0610
r_5	C_1–O_2^i	1.2642	–23.1546	–21.7689	30.4374	–14.4960	2.5327	0.0637
r_6	C_1–C_2	1.5580	–12.5798	–11.4664	9.9289	–14.1200	1.6635	0.0885

Table 4 Bond lengths R, Hessian eigenvalues λ_1–λ_3, electron density $\rho(r)$ and Laplacian $\nabla^2\rho(r)$ in BPC, calculated for anhydrous cobalt oxalate

CoC_2O_4		$R/\text{Å}$	$\lambda_1/\text{Å}^{-5}$	$\lambda_2/\text{Å}^{-5}$	$\lambda_3/\text{Å}^{-5}$	$\nabla^2\rho(r)/\text{Å}^{-5}$	$\rho(r)/\text{e}/\text{Å}^{-3}$	ε
r_1	Co–O_1	2.2351	6.3694	–0.9042	–1.0170	4.4490	0.3135	0.1247
r_2	Co–O_2^i	2.3045	–0.8008	5.2705	–0.6950	3.7740	0.2589	0.1522
r_3	Co–O_2^{ii}	2.4388	–0.6895	–0.5663	3.6848	2.4270	0.2015	0.2175
r_4	C_1–O_2^{ii}	1.2281	42.6798	–26.1959	–26.0513	–9.5790	2.7385	0.0056
r_5	C_1–O_1	1.2929	20.9375	–20.8338	–18.7878	–18.6840	2.4058	0.1089
r_6	C_1–C_2	1.5687	–11.9822	9.8349	–10.9097	–13.0570	1.6068	0.0983

$\rho(r)$ values, $\nabla^2\rho(r)>0$ and $|\lambda_1/\lambda_3|<1$). These parameters obtained for analyzed structures has been used in calculations of bond orders as defined by Cioslowski and Mixon [27] (improved by Howard and Lamarche [28]). The bond strains, according to the Bond Valence Method (an extensive review of BVM can be found in Brown [14]) have been calculated from structural data presented in Table 1. The detailed description of methods used in present calculations can be found in our previous paper [15].

Bond order

The concept of bond order has provided for generations of chemist a very useful tool to analyze and compare the relative strength of chemical bond. There are many different methods for calculating the bond order, both theoretical and experimental (recent review can be found in Jules and Lombardi [29]). Bader *et al.* [30] have defined following relationship between the bond order n_B, and the electron density in critical point ρ_{BCP}:

$$n_B = e^{A(\rho_{BCP} - B)}$$

The constants A and B in above formula has simple physical interpretation: $A = d\ln(n_B)/d\rho_B$ represents the fractional change in bond order, due to the unit change in electron density, and B is the electron density in the critical point for single bond ($n_B=1$). Another widely used, classical definition of bond order is due to Pauling [31] and is based on interatomic distances R only:

$$n_P = e^{\frac{r_0 - R}{a}}$$

where $r_0 = 1.521$ is an idealized single-bond length and $a = 0.293$. Both these definitions have limitations – Bader's formula gives reasonable good results for C–C bonds, but much worse for heterovalent bonds, while Pauling's bond order is not sufficiently sensitive to the bond environment, and electronic charge distribution. Nevertheless, they are often sufficient for qualitative analysis of bond orders.

Cioslowski and Mixon [27] have proposed another definition of bond order, called covalent bond order index, calculated from the properties of bond critical point. Their definition has been later improved by Howard and Lamarche [28] (they have fitted the parameters to generated set of the covalent bond-order data) and the respective formula can be expressed as:

$$n_{CM (HL)} = a_0 + a_1(\lambda_1 + \lambda_2) + a_2\lambda_3 + a_3\rho_{BCP}$$

where λ_1, λ_2, λ_3 – eigenvalues of the electron density Hessian matrix in bond critical point. Since the values ρ_{BCP} and λ_3 measure the σ character of the covalent bond, while the curvatures of the electron density perpendicular to the bond line, λ_1 and λ_2, measure the degree of its π character, this formula is suitable for different types of bonds. Therefore in our analysis we have used this last definition of bond order and respective values calculated for zinc, cadmium and cobalt oxalates are presented in Table 5.

Bond valence and bond strain

The use of empirical correlations between the bond length and strength of chemical bonds has a long history in crystal chemistry, starting from Pauling [31], Byström and Wilhelmi [32], Zachariasen [33] and Smith [34]. In 1970, Donnay and Allmann [35] suggested to use the notion 'bond valence' instead 'valence strength' proposed by Pauling. Bond valence and bond length are related by the inverse power relationship:

$$s_{ij} = (R_{ij}/R_0)^{-N}$$

where N and R_0 are the empirical constants, with R_0 being the length of a bond of unit valence. Another expression for the dependence $s(R)$, was suggested by Allmann [36] and Zachariasen [37]:

$$s_{ij} = e^{(R_0 - R_{ij})/b}$$

where R_0 has the sense of unit valence ($s_{ij}=1$), whereas b varies within a range from 0.32 to 0.48 Å. The present state of the art and perspectives of bond valence model in inorganic crystal chemistry has been reviewed by Urusov and Orlov [38] and Brown [14].

The 'experimental' s_{ij}^{exp} values can be easily calculated from the experimental bond lengths and the differences between the 'experimental' atomic valence $\sum s_{ij}^{exp}$ and the expected value V_i, calculated for an atom (d_i) or for entire structure (D):

$$d_i = V_i - \sum_j s_{ij}' \quad D = \sqrt{\langle d_i^2 \rangle}$$

can be used as a good measure of the reliability factor of the crystal structure. Larger values of d_i and D indi-

Table 5 Bond orders calculated from topological properties of electron density in bond critical points for chosen anhydrous oxalates

	MeC$_2$O$_4$	ZnC$_2$O$_4$	CoC$_2$O$_4$	CdC$_2$O$_4$
		$n_{CM(HL)}$	$n_{CM(HL)}$	$n_{CM(HL)}$
r_1	Me–O^1	0.95	0.85	0.89
r_2	Me–O^{2a}	0.91	0.83	0.86
r_3	Me–O^{2b}	0.84	0.82	0.86
r_4	C^1–O^1	1.60	1.25	1.16
r_5	C^1–O^{2a}	0.89	1.01	1.11
r_6	C^1–C^2	0.91	0.80	0.87

Table 6 Bond strain factors for individual bonds and the whole structure, calculated for chosen anhydrous oxalates, according to bond valence method

	ZnC_2O_4	CoC_2O_4	CdC_2O_4
δr_1 (Me–O^1)	0.1859	0.1029	0.0684
δr_2 (Me–O^{2a})	0.0541	0.1423	0.0091
δr_3 (Me–O^{2b})	0.1428	0.2005	0.0307
δr_4 (C^1–O^1)	0.2202	0.2156	0.1920
δr_5 (C^1–O^{2a})	0.3896	0.3666	0.0722
δr_6 (C^1–C^2)	0.0006	0.0746	0.0449
δ_{struct}	0.2074	0.2071	0.0911

cate the existence of strained bonds, which can lead to instabilities in the crystal and show most strained regions in the structure (which can simultaneously be the sites of the highest reactivity or liability). The difference between the theoretically predicted and experimentally observed bond lengths is another very useful indicator of bond strain. In this case, the strain factor δ for a certain group of bonds or the whole structure can be described by following formula:

$$\delta = \sqrt{\frac{\sum_{k=1}^{N_{bonds}}(s_{ij,k}^{theor}-s_{ij,k}^{exp})^2}{N_{bonds}}}$$

While d_i indicates the magnitude of unbalanced charge for given atom in the structure, the strain factors δ provide us additional information about the differences in strains acting on single bonds or group of bonds. Detailed results of bond valences, d_i and D factors for analyzed structures can be found elsewhere [15-17]. In this paper, we have focused only on bond strain factors, as ones directly related to bond properties and thus most important for our current analysis. In Table 6 the results of the calculations of respective bond strains factors are presented.

Discussion

The obtained results allow us to draw some conclusions concerning the relations between respective bonds properties and the way of thermal decomposition in given oxalate. In case of zinc oxalate the value of electron density in bond critical point BCP is largest for C^1–O^1 bond, then smaller but comparable in value for C^1–O^{2a} and C^1–C^2 bonds and much smaller for zinc oxygen bonds, but again greater for Zn–O^1 and smaller for both Zn–O^2 bonds. Thus the C^1–O^1 bond is the strongest one, the strength of C^1–O^{2a} and C^1–C^1 bonds is similar and the weakest bonds are created by zinc and oxygen atoms (Table 2). This allows us to suppose, that during thermal

decomposition process, as the first one, the one of the two longest Zn–O^{2b} bonds will be broken. Since O^{2b} atom is corner-shared by two octahedra (full analysis can be found in [16]), this will be followed by the process of shortening (and thus strengthening) of Zn–O^{2b} and C–O^{2b} bonds in second, neighboring octahedron in which O^{2b} atom remains and in the same time, the electron flow and substantial change in electron charge distribution in first octahedron and strengthening of Zn–O^{2a} and Zn–O^1 bonds (the first one to greater extent than the second one). Since the C^1–O^{2a} bond is slightly stronger than C^1–C^2 bond, taking all of this into account, we may assume the following sequence of consecutive bond breaking: Zn–O^{2b}, C^1–C^2 and Zn–O^1 (O^1 from neighboring octahedron, bonded to C^1 from analyzed octahedron) and as the result – free CO$_2$ molecule is created. The bond order analysis provides us some extra clarification, concerning the next steps of decomposition process (Table 5): the bond orders of C^1–O^{2a}, Zn–O^1 and Zn–O^{2a} are comparable (Zn–O bonds orders are slightly greater than the one for C^1–O^{2a}) and we can suppose, that as a next ones, the C^1–O^{2a}, than Zn–O^1 bonds will be broken, leaving Zn–O^{2a} and C^1–O^1 bonds unbroken. Eventually this process will lead to the decomposition of the anhydrous zinc oxalate to ZnO+CO+CO$_2$, in agreement with the experiment. The overall strains in the structure are significant (Table 6), and the highest strains act on C–O^2 bonds. The strains acting on Zn–O bonds are much smaller and comparable to C–O^1 bond strains. Thus it follows, that energetically most favorable should be breaking or resizing of the C–O^2 bond, which is in agreement with above analysis.

For cadmium oxalate (Table 2) we have the highest electron density concentration in carbon oxygen bonds; the lesser concentration is in C–C bonds and the least in metal oxygen bonds. The C–O and C–C bonds show covalent, while metal–oxygen bonds the ionic-covalent character. As the consequence, the strongest bonds in these structures should be C–O bonds, followed by C–C bonds and weakest and most easily breakable are Cd–O bonds. Similar picture emerges from bond order data (Table 5), except that calculated bond orders of Cd–O and C–C bond are comparable. The bond strain factors are small (Table 6) – the highest ones are for C–O bonds. These BVM results, bearing in mind the respective bond orders, allow us to state, that since C–O bonds are the strongest ones and in the same time most strained, and Cd–O are the weakest – during thermal decomposition process most probably metal–oxygen bonds will be broken as the first one, resulting in immediate relaxation of respective carbon–oxygen bonds. After that the carbon–carbon bond will break and as a result, the final products of thermal decom-

position will be cadmium and carbon dioxide, in agreement with experiment.

In cobalt oxalate case the obtained results are ambiguous, since electron density topological data, and derived bond orders are very similar to the ones obtained for cadmium oxalate, which suggests that this oxalate should decompose thermally to cobalt and carbon dioxide. On the other hand, the calculated bond strains are big, just the opposite to cadmium oxalate and are similar to bond strains obtained for zinc oxalate and thus one can suppose, that decomposition process should lead to cobalt oxide, carbon oxide and carbon dioxide. In our opinion this contradiction is only apparent, since these results indicate the sensitivity of this structure and bond properties to external strains, namely in case of polycrystalline sample, there can be different local strains due to grain boundaries, point and linear defects etc. and as a result, in some places strains can be reduced (leading to decomposition like in cadmium oxalate) and in the same time, in other places the strains can be increased (and this factor may dominate and results in decomposition as in case of zinc oxalate). This potential behaviour is confirmed by experiment – during thermal decomposition process, cobalt oxalates decompose via both ways (to a) cobalt and carbon dioxide and b) cobalt oxide, carbon oxide and carbon dioxide). Therefore, even if we are unable to predict unambiguously the way of thermal decomposition in this compound, we can infer a conclusion that from the point of view of the presented results (which are obtained for ideal crystal), both ways are probable and which one will actually be chosen depends on other factors like microstructure, point and 2D defects etc.

Conclusions

The main purpose of this paper was to show the possibility of the application of theoretical methods based on electron density topology to the analysis of structure and bonding properties, which allows us to describe and explain the behaviour of given compound during the thermal decomposition process. Presented results allow us to draw the conclusions, that topological analysis of the electron density can be treated as relatively simple and useful tool for describing bond properties in crystals. Theoretical analysis, if based on bond orders solely, leads to unambiguous results only when internal strains are small. In highly strained environment, bond breaking changes significantly nature of remaining bonds in a way difficult to predict and in such cases the topological analysis can be supported by the knowledge concerning bond strains calculated within Bond Valence Method, which allow us to predict the most probable direction

of charge flow and bond shortening/lengthening, thus their strength change. The results presented here show, that such complementary methods applied to the analysis of the crystal structure and bonding properties, allow us to describe, explain and to some extent also to predict the most probable way of thermal decomposition process for given structure, and hence can be considered as very promising additional tool in thermochemical analysis. In case of isostructural crystals, when more results are available, we can safely assume that if some initial crystal properties are similar, the way of thermal decomposition will also be similar. Hence even in some ambiguous cases, like anhydrous cobalt oxalate, we are able to postulate the most probable way of thermal decomposition.

Acknowledgements

References

1 Y. D. Kondrashev, V. S. Bogdanov, S. N. Golubev and G. F. Pron, Zh. Struct. Khim., 26 (1985) 90.
2 E. Jeanneau, N. Audebrand and D. Louer, Acta Cryst., C57 (2001) 1012.
3 B. Małecka, E. Drożdż-Cieśla and A. Małecki, Thermochim. Acta, 423 (2004) 13.
4 M. E. Brown, D. Dollimore and A. K. Galwey, Comprehensive Chemical Kinetics, Vol. 22. Reactions In Solid State, C. H. Bamford and C. F. H. Tipper, Eds, Amsterdam, Elsevier 1980.
5 V. V. Boldyrev, I. S. Nevyantsev, Y. I. Mikhailov and E. F. Khayretdinov, Kinet. Katal., 11 (1970) 367.
6 H. J. Borchardt and F. Daniels, J. Am. Chem. Soc., 79 (1957) 41.
7 D. Dollimore, Thermochim. Acta, 117 (1987) 331.
8 B. S. Randhawa and M. Kaur, J. Therm. Anal. Cal., 89 (2007) 251.
9 A. K. Galwey and M. E. Brown, J. Therm. Anal. Cal., 90 (2007) 9.
10 J. Fujita, K. Nakamoto and M. Kobayashi, J. Phys. Chem., 61 (1957) 1014.
11 S. Rane, H. Uskaikar, R. Pednekar and R. Mhalsikar, J. Therm. Anal. Cal., 90 (2007) 627.
12 R. F. W. Bader, Atoms in Molecules: A Quantum Theory, Clarendon Press, Oxford 1990.
13 L. Pauling, J. Am. Chem. Soc., 51 (1929) 1010.
14 I. D. Brown, The Chemical Bond in Inorganic Chemistry. The Bond Valence Model, Oxford University Press, 2002.
15 A. Koleżyński and A. Małecki, J. Therm. Anal. Cal., 96 (2009) 161.
16 A. Koleżyński and A. Małecki, J. Therm. Anal. Cal., 96 (2009) 167.
17 A. Koleżyński and A. Małecki, J. Therm. Anal. Cal., DOI: 10.1007/s10973-008-9494-0.

18 P. Blaha, K. Schwarz, G. K. H. Madsen, D. Kvasnicka and J. Luitz, WIEN2k, An Augmented Plane Wave+Local Orbitals Program for Calculating Crystal Properties (Karlheinz Schwarz, Techn. Universität Wien, Austria), ISBN 3-9501031-1-2, (2001).

19 J. C. Slater, Phys. Rev., 51 (1937) 151.

20 T. L. Loucks, Augmented Plane Wave Method, Benjamin, New York 1967.

21 O. K. Andersen, Solid State Commun., 13 (1973) 133.

22 D. R. Hamann, Phys. Rev. Lett., 42 (1979) 662.

23 E. Wimmer, H. Krakauer, M. Weinert and A. J. Freeman, Phys. Rev., B24 (1981) 864.

24 D. J. Singh, Planewaves, Pseudopotentials and the LAPW Method, Kluwer Academic Publishers, Dordrecht 1994.

25 J. P. Perdew, K. Burke and M. Ernzerhof, Phys. Rev. Lett., 77 (1996) 3865.

26 A. Koleżyński, E. Cieśla-Drożdż and B. Handke, sent to Acta Cryst. C.

27 J. Cioslowski and S. T. Mixon, J. Am. Chem. Soc., 113 (1991) 4142.

28 S. T. Howard and O. Lamarche, J. Phys. Org. Chem., 16 (2003) 133.

29 J. L. Jules and J. R.Lombardi, J. Mol. Struct. (Teochem), 664–665 (2003) 255.

30 R. F. W. Bader, T. S. Slee, D. Cremer and E. Kraka, J. Am. Chem. Soc., 105 (1983) 5061.

31 L. Pauling, The Nature of the Chemical Bond, Cornell University Press, Ithaca, New York 1960.

32 A. Byström and K. A.Wilhelmi, Acta Chem. Scand., 5 (1951) 1003.

33 W. H. Zachariasen, Acta Cryst., 7 (1954) 795.

34 J. V. Smith, Am. Mineral., 38 (1953) 643.

35 G. Donnay and R. Allmann, Am. Mineral., 55 (1970) 1003.

36 R. Allmann, Monatsh. Chem., 106 (1975) 779.

37 W. H. Zachariasen, J. Less-Common Met., 62 (1978) 1.

38 V. S. Urusov and I. P. Orlov, Crystall. Rep., 44 (1999) 686.